# BENDING CHARACTERISTICS OF CUSTOM CLT LAYUPS LAMINATED WITH PONDEROSA PINE HARVESTED FROM RESTORATION PROGRAMS

*Sina Jahedi*†

Graduate Research Assistant
E-mail: sina.jahedi@oregonstate.edu

*Lech Muszynski**†

Professor
E-mail: lech.muszynski@oregonstate.edu

*Mariapaola Riggio*†

Associate Professor
E-mail: mariapaola.riggio@oregonstate.edu

*Sujit Bhandari*†

Graduate Research Assistant
Department of Wood Science and Engineering
Oregon State University
Corvallis, OR 97331
E-mail: sujit.bhandari@oregonstate.edu

(Received October 13)

**Abstract.** National forest restoration programs aimed at effective mitigation of catastrophic wildfires and pest outbreaks in the Western region of the United States yield a substantial amount of small-diameter ponderosa pine logs. Lumber produced from these logs is considered low-value due to lower mechanical properties compared with commercially harvested lumber. The US Forest Service is seeking a value-added market for this material to offset the high costs of forest restoration operations. Cross-laminated timber (CLT) is considered one potential market for the material. This study was part of a larger project to determine the feasibility of utilizing CLT fabricated from restoration harvested ponderosa pine in low-rise modular mass-timber construction. A CLT layup was designed based on the design requirements of a modular construction system determined in a parallel study. The bending characteristics of that layup were empirically verified through mechanical tests on prototype panels, three fabricated at a pilot-plant line at Oregon State University and two at an industrial manufacturing line. In all prototypes, grades No. 1, 2, 3, and ungraded laminations were assigned to all layers randomly. Standard ASTM D198 methods for long- and short-span flatwise bending tests were conducted to derive effective moment capacity, effective stiffness, and shear capacity of the layups. Optical measurement based on digital image correlation was used to derive effective shear rigidity of the specimens. There were no significant differences between results obtained from prototypes fabricated in the pilot plant compared with those fabricated in an industrial setting. Mechanical tests indicated that prototype CLT panels exceeded the structural requirements. Effective moment capacity, stiffness, and shear rigidity were higher than values estimated by the shear analogy method. Shear capacity was lower than predicted. Restoration program ponderosa pine CLT layups can be custom-designed to meet mechanical requirements for structural elements in certain classes of modular buildings.

***Keywords:*** Cross-laminated timber, forest restoration programs, low-value lumber, ponderosa pine, design values, bending stiffness, moment capacity.

* Corresponding author
† SWST member

*Wood and Fiber Science*, 55(3), 2023, pp. 282-294
https://doi.org/10.22382/wfs-2023-23

## INTRODUCTION

Forest restoration thinning programs are essential measures for mitigating catastrophic wildfires and pest outbreaks in the Western U.S. forest lands. In these operations, smaller and dead trees are selectively harvested to preserve larger and superior trees (Graham et al 1999). Restoration programs in the Pacific Northwest yield a substantial amount of ponderosa pine, *Pinus ponderosa*, (PP) lumber generated mostly from small-diameter logs, containing significant amounts of juvenile wood, wane, and prone to twist. The majority of that lumber is considered low-value (Rainville et al 2008) and is not typically used for structural purposes (Smith personal communication). United States Department of Agriculture (USDA) Forest Service is seeking a value-added market for PP lumber generated in restoration programs to offset the high costs of these operations.

Cross-laminated timber (CLT) is considered one potential market for such material (Lawrence 2017a). CLT is a structural engineered wood panel comprised of at least three orthogonal laminations of graded lumber bonded with a structural adhesive. The idea of utilizing low-grade lumber in engineered wood products is not a new concept. Research on small diameter yellow-poplar, *Liriodendron tulipifera* (Mohamadzadeh and Hindman 2015), fast-grown eucalyptus, *Eucalyptus grandis* (Liao et al 2017), Monterey pine, *Pinus radiata* (Sigrist and Lehmann 2014), and sugar maple, *Acer saccharum* (Ma et al 2021) demonstrated that low-grade lumber can provide satisfactory structural properties in CLT. PP lumber obtained from small-diameter trees can also be utilized in the fabrication of structural glue-laminated timber (Hernandez et al 2005). The feasibility of hybrid CLT panels consisting of structural grade lumber for outer layers and low-grade lodgepole pine, *Pinus contorta* (Larkin 2017), and mixed restoration harvested species including PP (Lawrence 2017b) in the inner layers was studied at Oregon State University (OSU). These studies demonstrated that the custom hybrid CLT panels had strength and stiffness comparable with E3 reference CLT grade as defined in PRG-320, which specifies the requirements for fabrication, performance, and quality assurance of CLT panels produced and used in North America (ANSI/APA 2019). This standard allows visually graded No. 2 or better lumber in layers aligned with the major strength direction of the panel, while No. 3 or better lumber can only be used in layers aligned with the minor strength direction of standard CLT panels. However, the standard permits custom layups as long as all laminations are visually or machine graded, and the CLT layup meets stipulated performance criteria.

Mechanical characteristics of CLT panels can be predicted based on the properties of laminations arranged in the layup. For this purpose, PRG-320 refers specifically to the shear analogy method (Kreuzinger 1999). The calculations are typically conducted based on reference design values published in the National Design Specification (NDS) supplement handbook (American Wood Council 2018) for commercially harvested lumber of species and species groups. In this document, the design characteristics for commercially harvested PP are provided as part of the “Western Woods” (WW) species group. However, previous studies indicate that the lumber harvested from restoration programs has lower mechanical properties compared with commercially harvested material due to the presence of substantially larger proportions of juvenile wood (Erikson et al 2000; Vaughan et al 2021; Jahedi et al 2022). Consequently, visually graded lumber harvested from restoration programs often does not meet the NDS design characteristics of similar grades (Erikson et al 2000; Hernandez et al 2005; Jahedi et al 2022). Instead, it has been proposed that the highest visual grade in NDS that actually matches the mechanical characteristics of the lumber generated in restoration thinnings could be used for designing custom CLT layups.

The next difficulty with using these materials is defining a structural application with the potential for utilizing substantial volumes of such CLT panels. The large size and weight precludes the custom-fabrication of mass timber panels on the construction site. Panels must be prefabricated for specific projects and there is no commodity market for unfinished mass timber panels. Current mass timber panel construction in North America is still focused on high-profile, often tall, and first-of-their-kind structures calling for high-grade CLT panels. However, low-rise modular structures may present a more appropriate outlet for panels composed of lower-grade lumber, by providing the chance to produce stock panels for a particular end-use, such as temporary classrooms, affordable housing units, or medium to long-term emergency housing.

Creating a prototype design of such modular structures specifically aimed at using CLT panels fabricated from restoration harvested PP was the focus of a parallel study that also assessed minimum mechanical characteristic requirements for the CLT panels to be used in such structures (Bhandari 2022; Bhandari et al 2024).

The goal of this study was to assess the mechanical characteristics of CLT panels composed of PP generated in forest restoration thinnings for specific applications in low-rise modular buildings. The specific objectives were to:

- Determine a custom layup for PP CLT that meets the design requirements of the modular structure proposed by Bhandari et al (2024).
- Experimentally quantify the relevant mechanical characteristics of the prototype panels fabricated based on that custom layup.
- Determine the impact of fabrication scale on the mechanical characteristics of the prototype panels.

## MATERIALS AND METHODS

The general approach of the study was to 1) design a CLT layup using the shear analogy method based on the requirements of the target structural design, and 2) experimentally verify the selected mechanical characteristics of the resulting CLT layups relevant for that type of structure. The focus was on standard long- and short-span flatwise bending tests in the major strength direction to derive effective moment capacity $F_bS_{\mathrm{eff},f,0}$, effective stiffness $EI_{\mathrm{eff},f,0}$, and shear capacity $v_{s,0}$. Strain fields in the shear span of the specimens were measured using an optical system to derive effective shear rigidity $GA_{\mathrm{eff},f,0}$. The edgewise and minor strength directions were not critical for the structural panel elements in the proposed design (Bhandari 2022; Bhandari et al 2024). The prototype CLT panels were fabricated following the theoretical layup design in two scales: in a pilot-line scale at OSU and a full-scale industrial setting at a DR Johnson Wood Innovations CLT manufacturing plant.

## DESIGN OF CUSTOM PP CLT LAYUPS

The shear analogy method (Kreuzinger 1999) as formulated in PRG-320, Appendix X3 (ANSI/APA 2019), was adopted in a computer application named Layup-App (Jahedi et al 2020), whose objective was to find a CLT layup with a minimum gross thickness that meets the structural requirements dictated by the modular building designed for this project. These requirements were the minimum allowable stress design (ASD) reference design values to satisfy the bending and shear criteria per NDS, short-term and long-term deflection criteria per IBC 2018 (ICC 2018), and vibration criteria per CLT Handbook for a 3.6 m (12 ft) span simply supported floor. A total dead load of 2.4 kN/m$^2$ (50 psf) including self-weight, and a live load of 1.9 kN/m$^2$ (40 psf) were considered in the analysis. The minimum building requirements are labeled as "Target Values" in Table 3.

As discussed earlier, NDS design characteristics for visually graded PP lumber could not be used directly for the material generated in restoration thinnings. A previous study analyzed modulus of elasticity (MOE) values of PP lumber from restoration thinnings performed in Southern Oregon and Northern California visually graded as No. 1, No. 2, No. 3, as well as ungraded lumber sawn mostly from dead trees (Jahedi et al 2022). Lumber graded as No. 1 (a marginal fraction of the analyzed lumber) and No. 2 did not meet the NDS MOE characteristics for respective visual grades of the WW species group which includes PP. However, average MOE values of all visual grades and the ungraded material were higher than NDS WW grade No. 3. No statistically significant difference was found in MOE values determined between visual grades No. 2, No. 3, and the ungraded lumber (Jahedi et al 2022). Hence, it has been proposed that the design characteristics of PP lumber from restoration thinnings could be conservatively assumed as corresponding to those of NDS WW No. 3. The authors further proposed that pooling restoration PP lumber regardless of the visually assigned grade for the purpose of designing project specific custom CLT layups could maximize material utilization and reduce production costs (Jahedi et al 2022). The current study examined whether any PP lumber meeting the minimum visual grade requirements of WW No. 3 could be used in the CLT layup. Consequently, the design values of WW grade No. 3 as presented in NDS, Table 4A (American Wood Council 2018), were used to represent the mechanical characteristics of restoration program PP laminations assigned for longitudinal and transverse directions.

A general flowchart of the Layup-App is shown in Fig 1. The approach started with a 3-ply CLT layup with the thinnest laminations permitted by PRG-320 (16 mm) and used the shear analogy method to calculate the design characteristics of the layup. Lamination thickness was increased by 3 mm if layup design characteristics were predicted to be lower than the design requirements, ie allowable $F_bS_{\mathrm{eff},f}$, $EI_{\mathrm{eff},f}$, $\nu_s$ and $GA_{\mathrm{eff},f}$. Two additional lamina were added where the model predicted lamination thicknesses exceeding 51 mm which is the maximum permitted by PRG-320 and the thickness of all laminations was set to 16 mm again. Although the Layup-App allows various thicknesses for each layer, the analysis was limited to symmetric layups with the same thickness for all layers to reduce manufacturing complications.

The solution best matching the structural design requirement was a 5-ply CLT 168-mm thick

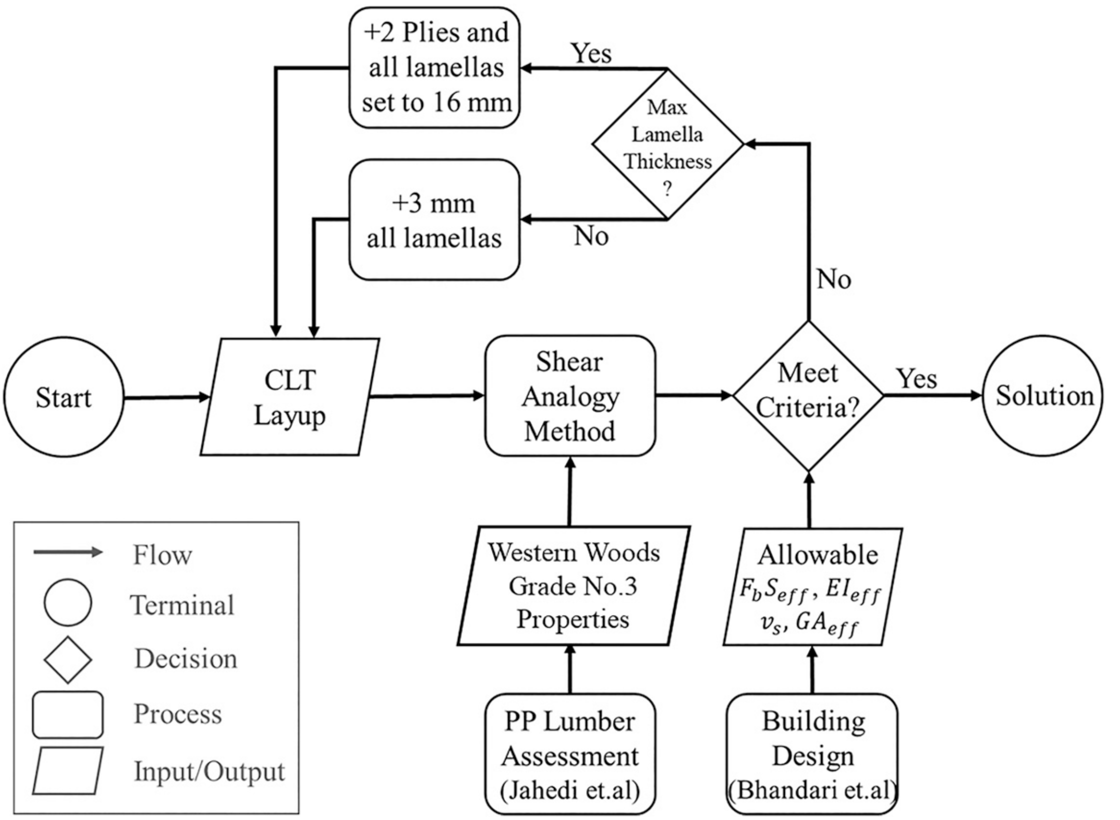


Figure 1. Flowchart of the Layup-App developed to find a CLT layup meeting the building requirements.

layup. This finding informed the next stage of the project for the fabrication of CLT prototypes. The design values of the layup are presented in Table 3, labeled as "Shear Analogy Est.", in the results section, and were compared with the experimentally derived design values.

#### FABRICATION OF PROTOTYPE PP CLT

The custom PP CLT prototypes were fabricated using $2 \times 6$ nominal dimension PP lumber obtained from Southern Oregon and Northern California restoration operations performed by Collins Co. (Lakeview, OR). A total of 63.7 $m^3$ (27,000 Bdft) of lumber was kiln dried and visually graded by the company: 50% of the material as No. 2 or better and 35% as No. 3. The remaining 15% of the material was sawn mostly from dead trees was delivered ungraded. The material was stored in a roofed outdoor shed in tight units in the original wrapping. The average MC of the boards determined at the time of the panel fabrication was 10.8% $\pm$ 1.1. One of the goals of this study was to investigate the impact of fabrication scale on the performance of the prototypes, therefore, samples were made in a laboratory and an industrial setting and were subjected to the same tests. Some of the lumber (7.4 $m^3$ or 3150 Bdft) was used to fabricate laboratory prototype (LP) panels at the A.A. 'Red' Emmerson Advanced Wood Products Laboratory, OR State University. The remainder (8.3 $m^3$ or 3500 Bdft) was sent to DR Johnson Wood Innovation, a CLT manufacturing plant located at Riddle, OR, to fabricate industrial prototypes (IP) panels.

Lumber for the LP prototypes was planned on four sides using a medium-scale industrial planner (LeaderMac, Blaine, WA) to achieve uniform thicknesses and to refresh the surfaces for good bonding. For optimal performance, the machine was equipped with brand-new cutting blades. PRG-320 states that thickness variations across the width of lumber shall not exceed $\pm$0.20 mm in every 305 mm width and $\pm$0.30 mm along the length. The lumber thickness of 12 specimens was measured immediately after planning using a $\pm$0.01 mm caliper at 36 points along the length on each edge of the lumber, 72 measurement points per specimen. The average of measured variations across the lumber width was 0.04 mm (with a standard deviation of 0.11 mm and a maximum of 0.41 mm), and the average variation along the length was 0.01 mm (with a standard deviation of 0.09 mm and a maximum of 0.83 mm). Eight of 12 specimens failed to meet the PRG-320 thickness tolerances criteria in one or multiple points and were excluded from production. No data on lamination thickness variation were available for the panels made by the industrial partner. All laminations were planned within 48 h of production.

LP and IP lumber pieces from all graded groups and the ungraded group were assigned to all layers randomly. The 5-ply prototype layups were bonded using a two-component melamine formaldehyde adhesive system (AkzoNobel 1263_9563; Amsterdam, the Netherlands). Fabrication factors were set as per the adhesive manufacturer's guidelines. For the LP sample, adhesive was spread by a custom pilot-line scale adhesive applicator with a spread rate set to 340 g/$m^2$ and a resin-to-hardener ratio of 100:100. The layups were pressed for 3 h under a 0.68 MPa pressure using a pilot-plant scale Minda press. The IP samples were produced using fabrication adhesive spread rates, open times, and pressures similar to a typical production at that plant; however, the exact values were not disclosed.

The specimens required to conduct the targeted mechanical tests were obtained from three 2.43 m by 3.05 m LP 5-ply CLT panels and two 3.05 m by 5.49 m IP 5-ply CLT panels with major direction oriented parallel to the grain (Table 1). While PRG-320 specifies a span-to-depth ratio of 30 for long-span bending tests, the achievable ratio for the LP sample was restricted by the size of the CLT press in the pilot plant which only allowed the fabrication of panels up to 3.05 m in length.

The goal of three-point bending tests was to measure the rolling shear strength of the panels. That is why PRG-320 and ASTM D198 specify a relatively small span-to-depth ratio (between 5 and 6) to ensure rolling shear failure, rather than failure

Table 1. Summary of the tests performed, number of specimens, and dimensions.

| Type of tests | Sample group | No. of specimens | PRG-320 span/depth | This study span/depth[a] | Length, width and depth mm × mm × mm |
|---|---|---|---|---|---|
| Third-point bending | LP | 11 | 30 | 17.2 | 3040 × 300 × 168 |
| | IP | 14 | 30 | 30.6 | 5483 × 300 × 174 |
| Three-point bending | LP | 6 | 5 to 6 | 6.0 | 1158 × 300 × 168 |
| | IP | 16 | 5 to 6 | 5.5 | 1114 × 300 × 174 |

[a]Half of the bearing support (76 mm from each side) was deducted from the actual length when the span was calculated.
LP, laboratory prototype; IP, industrial prototype.

in bending. The short-span LP specimens were cut with a span-to-depth ratio equal to 6 and it was observed that half of them failed in bending, and their ultimate rolling shear strength remained unknown. Therefore, the span-to-depth ratio of IP specimens was reduced to 5.5 to ensure rolling shear failure.

Visual inspection revealed the presence of preexisting interlaminar gaps in 15 (88%) of LP and 23 (76%) of IP bending specimens. On average, interlaminar gaps covered 0.9% of the bond line perimeter of LP and 1.8% of the IP bending specimens. Bond integrity test samples are reported separately and showed that these gaps were the main cause for poor resistance to delamination (Jahedi et al 2023). In addition, that study isolated the impact of adhesive/species compatibilities and demonstrated that interlaminar gaps were caused by fabrication issues, which could include excessive thickness variations within laminations, uneven clamping pressure, or a combination of both.

## MECHANICAL TESTS

All tests performed in this study are summarized in Table 1. The third-point bending test method specified in ASTM D198 standard, sections 4 through 12, was followed to determine flatwise effective moment capacity $F_bS_{eff,f,0}$ and effective stiffness $EI_{eff,f,0}$. Three-point bending tests were conducted on short beams following the same standard to derive flatwise shear capacity $v_{s,0}$. In both types of tests, an Linear Variable Differential Transformer (LVDT) sensor was installed on a yoke suspending from the reaction points to measure the total deflection of the neutral axis at the center of the beams. A second LVDT sensor was used in the third-point bending test to measure the deflection of the neutral axis in the shear-free span between the loading points. An optical measurement system based on the digital image correlation (DIC) principle, by Correlated Solutions (Schreier et al 2009), was used to measure the shear strains $\varepsilon_{xy}$ in the shear span to determine flatwise effective shear rigidity $GA_{eff,f,0}$, Fig 2.

Mechanical properties were derived using equations presented in ASTM D198, Table X2.1. A load duration adjustment factor ($C_D = 1.6$) was applied to the maximum shear and bending loads to compensate for the actual duration of the tests (10 min) compared with 10 yr live load duration used to derive shear analogy values. Additionally, 5th percentile tolerance limit of the data divided by a safety factor ($C_{ASD} = 2.1$) was considered to derive strength-related design values, ie $F_bS_{eff,f,0}$ and $v_{s,0}$, (ANSI/APA 2019). While the number of specimens fabricated and tested in this study met the standard requirements, the sample size was too small to determine the 5th percentile datapoint directly from the pooled data. However, for normally distributed data, it is possible to calculate the 5th percentile tolerance limit from Eq 1, where $\mu$ is the mean and $\sigma$ is the standard deviation of the data. The normality of the data was confirmed using the Shapiro–Wilk method which is suitable for sample sizes smaller than 20 (Mishra et al 2019). This procedure was also applied to very sparse LP datasets even though the outcome was expected to carry limited statistical significance.

$$x_{5th\ percentile} = \mu - 1.64\ \sigma \quad (1)$$

Averages of respective measured values for all specimens were used for deflection-related design

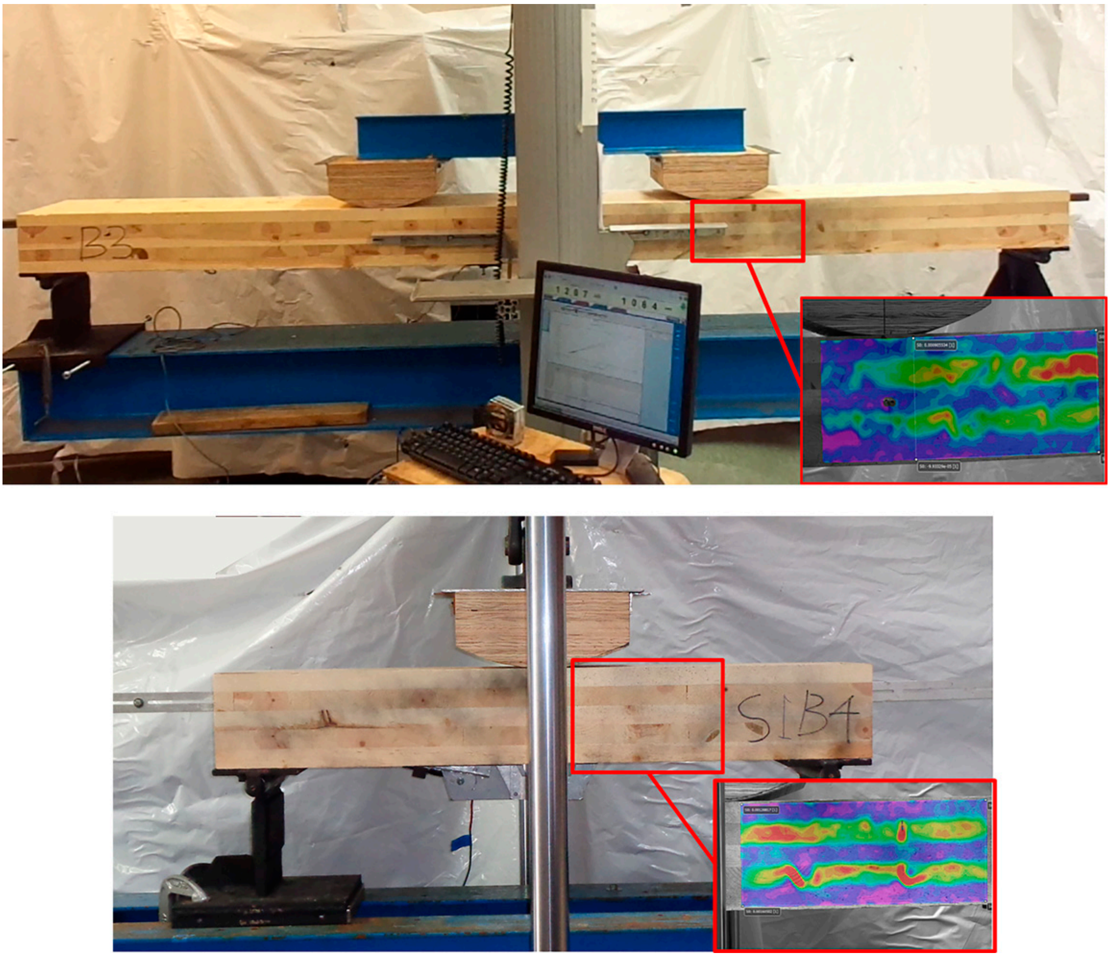


Figure 2. Third-point (top) and 3-point (bottom) bending test setups. The field of view of the optical system is marked in red. LVDT sensors that were extended through the length were installed behind the beams and not shown in the images.

values, ie $EI_{\mathrm{eff},f,0}$ and $GA_{\mathrm{eff},f,0}$. In PRG-320, the ASD reference design values are presented per a unit of width, ie per 1 ft of the width of the structural element. For consistent use of the metric system, these design values were converted from 1 ft of width to 1 m of width. The application of the adjustments is summarized in the set of Eqs 2-5:

$$\text{Effective moment capacity}: \; F_b S = \frac{F_b S_{5\%}}{C_D \, C_{\mathrm{ASD}}} \tag{2}$$

$$\text{Effective stiffness}: \; EI = EI_{\mathrm{av}} \tag{3}$$

$$\text{Effective shear capacity}: \; v_s = \frac{v_{s\,5\%}}{C_D \, C_{\mathrm{ASD}}} \tag{4}$$

$$\text{Effective moment capacity}: \; GA = GA_{\mathrm{av}} \tag{5}$$

The average shear strain of the specimens through the entire beam depth was acquired from the shear span of the beam (Fig 2). The area of interest in the camera view was located 10 mm from the load point to avoid the impact of stress concentration around the load point on the results. The average of shear strain $(\varepsilon_{xy\ av})$ in all measurement points within the area of interest spaced 7 pixels apart were used in Eq 6 to derive effective shear moduli, $G_{\mathrm{eff},f,0}$, of the beams where, $\tau_{av}$ is the average shear stress on the cross section of the beam, $P$ is the total load force exerted, $b$ is the width, and $h$ is the depth of the beam.

$$G_{\mathrm{eff},f,0} = \frac{\tau_{\mathrm{av}}}{\varepsilon_{xy\ \mathrm{av}}} \quad (6)$$

$$\tau_{av} = \frac{P}{2\,b\,h} \quad (7)$$

## RESULTS

The modulus of elasticity (MOE), true elastic modulus ($E_{\mathrm{true}}$), shear modulus, (G), and the modulus of rupture (MOR) of prototype custom PP CLT samples determined in the third-point bending and the three-point bending on short beams are presented in Table 2.

Average MOR values for short beams tested in three-point bending include nominal MOR values of the specimens that failed in rolling shear as well as those that failed in flexure. However, the short beam specimens that failed in flexure were not included to derive the shear capacity design values.

The cumulative distributions of experimentally derived values were compared with the ASD reference design values estimated through the shear analogy method (Figs 3-6). The triangles and circles represent data points belonging to individual specimens for LP and IP groups, respectively, values are presented with safety and adjustment factors applied. Design values of basic grade E3 CLT with a similar layup are included in the graphs for comparison.

Even though it is more common to fit strength data with Weibull or lognormal distributions, given the limited scope of this study, normal distribution of properties was assumed. Shapiro–Wilk tests showed that all groups, except shear rigidity for the long-span IP group, met the normality criteria; therefore, cumulative normal distribution lines were fitted to the data, as shown in Figs 3-6. The intersection of the 5th percentile horizontal lines for moment and shear capacity and the 50th percentile for stiffness and shear rigidity with the fitted normal distribution lines indicate the reference design values for each group. For consistency of the presentation, this procedure was also applied to sparse LP datasets shown in Figs 4 and 5, even though the outcome carries very limited statistical significance.

The experimental design values at the 5th percentile tolerance limit for strength-related properties were determined numerically using Eq 1 and adjustment factors were applied. The design values for deflection-related properties were calculated as the mean values of the experimental data, following PRG-320. The results are summarized in Table 3.

One-way ANOVA tests ($\alpha = 0.05$) of test data of bending samples showed that the outcomes of IP and LP did not differ significantly in any group. This outcome suggests that the scale of the fabrication line (pilot-plant vs industrial) does not have a significant impact on the bending properties of PP CLT billets.

## DISCUSSION

The experimentally derived bending characteristics met the structural requirements of the reference

Table 2. Summary of effective mechanical properties of PP CLT prototype specimens.

| | | MOE | | $E_{\mathrm{true}}$ | | G[a] | | MOR | |
|---|---|---|---|---|---|---|---|---|---|
| | | GPa | | GPa | | GPa | | MPa | |
| Bending test | Sample | Avg | Std | Avg | Std | Avg | Std | Avg | Std |
| Third-point | LP | 6.0 | 0.5 | 6.3 | 0.5 | 0.47 | 0.12 | 21.7 | 4.3 |
| | IP | 4.4 | 0.5 | 5.2 | 0.5 | 0.40 | 0.17 | 17.7 | 2.7 |
| Three-point test | LP | 6.0 | 0.6 | — | — | 0.44 | 0.11 | 25.1 | 3.5 |
| | IP | 2.5 | 0.2 | — | — | 0.37 | 0.05 | 19.3 | 1.0 |

No safety factors were applied to the values.

[a]Shear modulus values were calculated using DIC optical measurements.

CLT, cross-laminated timber; DIC, digital image correlation; PP, ponderosa pine.

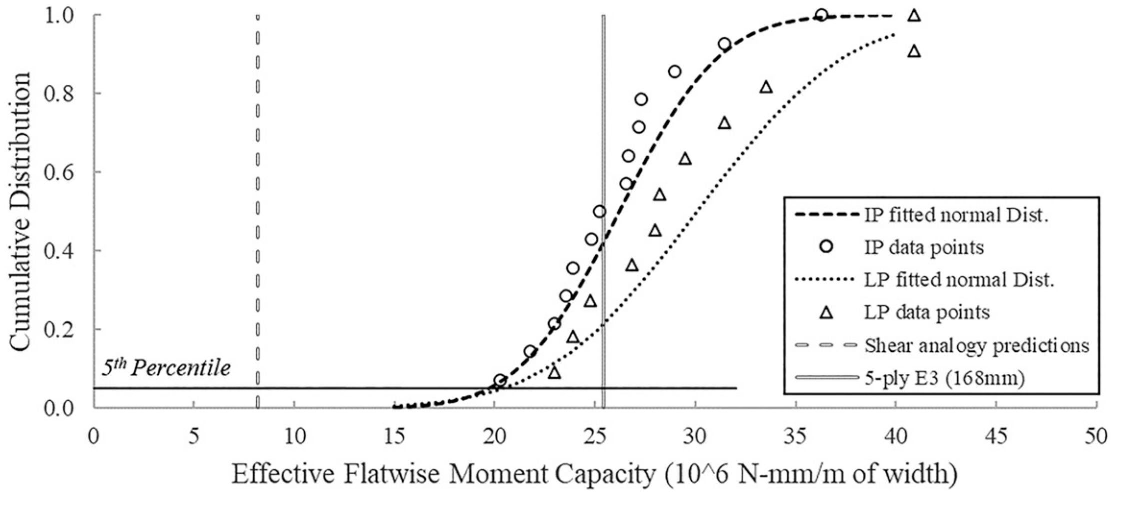


Figure 3. Cumulative distribution of experimentally derived effective flatwise moment capacity values compared with shear analogy estimates and basic E3 CLT grade with the same layup.

modular project. The effective moment capacity, effective stiffness, and effective shear rigidity design values for IP and LP exceeded the shear analogy estimates calculated using NDS reference design values for WW No. 3 lumber. However, the experimental shear capacity design values were about 40% lower than the shear analogy estimates. The findings partially validate the hypothesis that the PP lumber from forest restoration thinnings pooled in one group regardless of the visual grade assignment can be considered as a standalone material class, and that NDS WW grade No. 3 conservatively represents the mechanical properties. However, defining such pooled grade for lumber generated from small logs harvested in restoration projects would require the determination of the statistical distribution of MOE in larger samples derived from a representative number of stands and

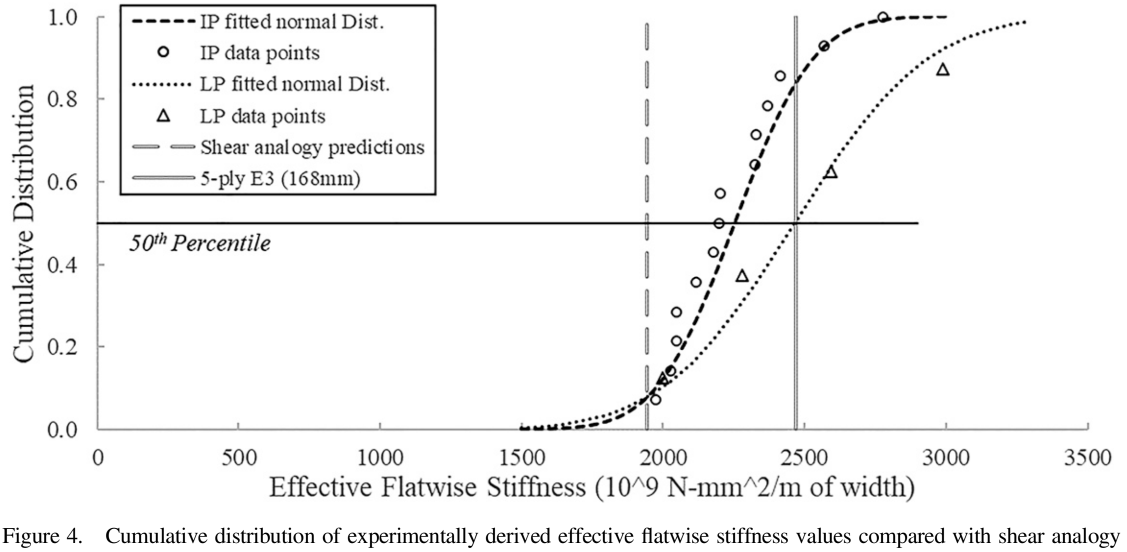


Figure 4. Cumulative distribution of experimentally derived effective flatwise stiffness values compared with shear analogy estimates and basic E3 CLT grade with the same layup.

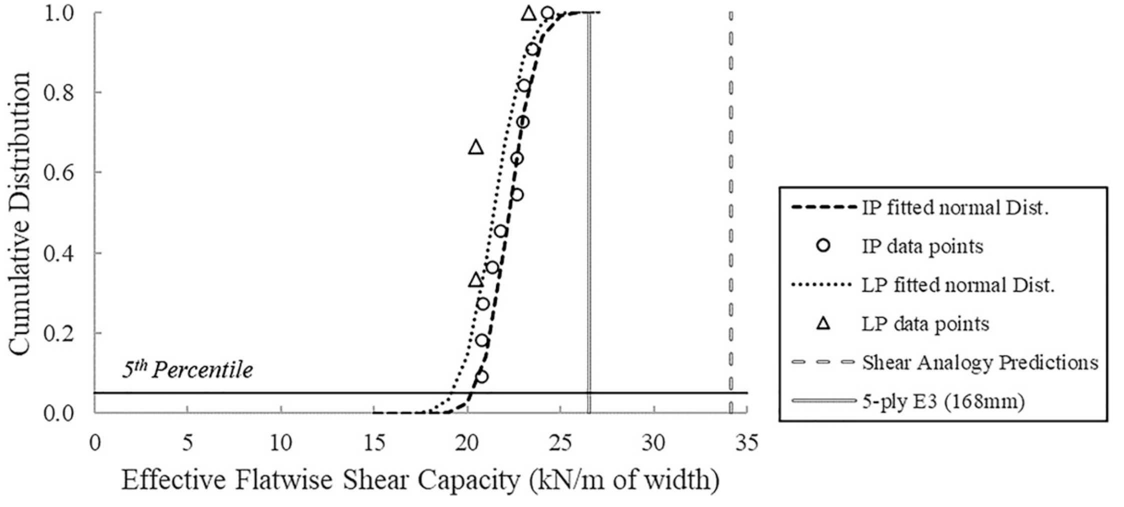


Figure 5. Cumulative distribution of experimentally derived effective flatwise shear capacity values compared with shear analogy estimates and basic E3 CLT grade with the same layup.

a determination of reliable correlation between MOE and MOR in these samples.

One potential reason for the low-shear capacity may be the presence of interlaminar gaps detected in 80% of the specimens. These gaps led to delamination failures in standard bond integrity tests observed in a parallel study conducted within this project (Jahedi et al 2023). The interlaminar gaps may have resulted from a combination of high thickness variations along the laminations and uneven clamping pressure.

Large differences (by a factor of *x*7.8 for LP and *x*7.1 for IP) were observed between the shear rigidity design values derived empirically and the shear analogy estimates. The differences may reflect the assumption used in the formulation of the shear analogy method referred to in PRG-320 of a proportional relationship between the shear

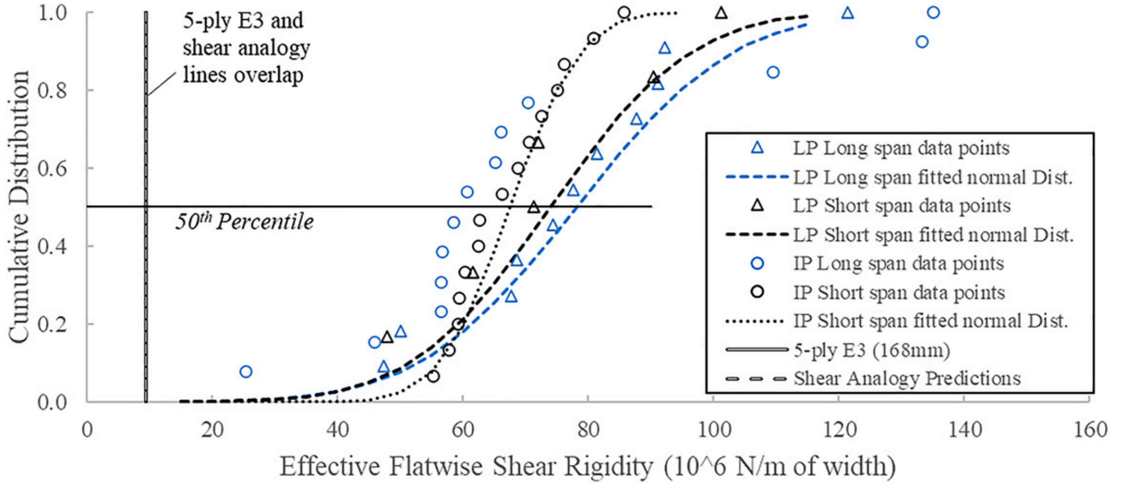


Figure 6. Cumulative distribution of effective flatwise shear capacity values derived from short- and long-span (third-point and three-point) bending tests compared with shear analogy estimates and basic E3 CLT grade with the same layup.

Table 3. Summary of theoretically and empirically derived effective flatwise ASD reference design values of restoration program PP CLT in the major strength direction.

| | Moment capacity $F_bS_{eff,f,0}$ | Stiffness $EI_{eff,f,0}$ | Shear rigidity $GA_{eff,f,0}$ | | Shear capacity $v_{s,0}$ |
|---|---|---|---|---|---|
| **Numerically derived** | $10^6$ N-mm/m | $10^9$ N-mm$^2$/m | $10^6$ N/m | | kN/m |
| Target values[a] | 7.4 | 1262 | 4.3 | | 8.0 |
| E3 basic grade | 25.4 | 2469 | 9.5 | | 26.5 |
| Shear analogy estimates | 8.2 | 1941 | 9.5 | | 34.1 |
| **Experimentally derived** | | | Long-span | Short-span | |
| LP | 20.4 | 2465 | 78.1 | 74.1 | 19.3 |
| IP | 19.7 | 2254 | 72.3 | 67.6 | 20.3 |

All design values are ASD references. Safety and adjustment factors per PRG-320 were applied to the values above.

[a]The minimum design values requirements for the building designed for this project.

ASD, allowable stress design; LP, laboratory prototype; IP, industrial prototype; CLT, cross-laminated timber; PP, ponderosa pine.

modulus $G_0$ and the elastic modulus $E_0$ in the longitudinal direction, to be $G_0 = E_0/16$ for all species. The rationale for this assumption dates back to the 1970s when experiments on clear specimens suggested that the proportion between shear modulus and true elastic modulus fell between 1/12 and 1/20 (Samson and Sotomayor-Castellanos 1991). However, the ratio for clear PP specimens reported in the FPL 2010 Wood Handbook is 1/7 (Kretschmann 2010), which is significantly larger than the 1/16 ratio assumed in PRG-320 for all species. Furthermore, this assumption should not be applied to strength-graded lumber, where the characteristic elastic modulus is affected by grade-defining characteristics, such as number, size, and position of knots and slope of grain. In fact, empirical studies suggest that shear modulus in dimension lumber is independent of lumber grade (Khokhar et al 2008).

While characteristics derived experimentally in this study were closer to the actual characteristics of the layup, it shall be noted that the shear analogy method is recognized as a primary practice to calculate the reference design values of custom CLT layups in PRG-320. The mechanical tests were meant to validate the characteristics derived from the shear analogy method. Therefore, shear analogy estimates for effective moment capacity, stiffness, and shear rigidity determined in this study (Table 3) could be used as provisional primary design characteristics for engineering purposes. However, the experimental shear capacity value (19.3 kN/m) may be a better estimate of the ASD reference design value than the shear analogy prediction.

## Limitations

One of the limitations of this study was that the material on which the MOE was determined was used to build the specimens for this project. Therefore, the exact correlation between MOE and MOR or other properties of the restoration program Pacific PP that would require destructive tests could not be determined in this project and must be assumed unknown. Determination of this correlation should be the subject of a future study.

The limited scope of this study provides an important context for the interpretation of the results. For simplicity, all datasets were processed as normally distributed, even though the normal distribution was clearly not a good fit for one group of the specimens (IP). Similarly, for consistency of presentation, shear and stiffness characteristics for the LP group were determined using distributions fitted to sparse datasets, even though the values obtained that way carry limited statistical significance. These limitations, however, do not invalidate the proof of concept discussed here, that is the demonstration of the potential for custom PP CLT layup to satisfy the demands of a specific type of modular construction. Actual structural use would require such layups to be properly certified.

## CONCLUSIONS

A custom CLT layup meeting the requirements of a low-rise modular building design was determined using an iterative algorithm based on the shear analogy method. The design values were derived assuming PP lumber harvested from restoration programs in Southern Oregon and Northern California will be used in all layers regardless of assigned visual grades.

Prototypes of the resulting CLT layup with random grade assignment in all layers were fabricated at a pilot plant at the OSU and on an industrial line operated by a commercial CLT manufacturer. All empirically determined design bending characteristics met the requirements of the reference modular building. The effective moment capacity, stiffness, and shear rigidity of layups produced in both types of facilities was higher than the design values estimated with the shear analogy method. However, the shear capacity was substantially lower than the estimated value.

Substantial discrepancy between experimentally derived shear capacity and shear analogy method estimates can likely be attributed to the interlaminar gaps detected in 80% of specimens. For specimens fabricated at the pilot-scale line, the gaps may have resulted from a combination of poor thickness tolerance of the laminations and uneven clamping pressure distribution. However, there is no sufficient evidence to explain the existence of interlaminar gaps in panels fabricated in the industrial CLT line.

The fact that the shear analogy method underestimated the shear rigidity of CLT layups was likely related to the assumed universal proportional relationship between shear modulus and elastic modulus for all softwood species and lumber grades based on correlations found in small clear specimens.

It is concluded that the restoration program PP CLT layups can be custom designed to meet mechanical requirements for structural elements in certain classes of modular buildings.

## ACKNOWLEDGMENTS

The work upon which this paper is based was funded in whole through a grant awarded by the U.S. Forest Service, Wood Innovations program 17-DG-11062765-742 and 18-DG-11062765-738. The Authors also wish to acknowledge the partnership of Tallwood Design Institute, and in-kind support from Collins Co., AkzoNobel, and D.R. Johnson Wood Innovations.

## REFERENCES

American Wood Council (2018) NDS supplement national design specification design values for wood construction. Leesburg, VA.

ANSI/APA (2019) ANSI/APA PRG 320:2019 Standard for performance-rated cross-laminated timber. Tacoma, WA.

Bhandari S (2022) Modular cross laminated timber structures using underutilized Ponderosa pine. PhD dissertation, Oregon State University, Corvallis, OR. 175 pp.

Bhandari S, Fischer EC, Riggio M, Muszynski L, Jahedi S (2024) Mechanical characterization of connections for modular cross laminated timber construction using underutilized lumber. ASCE J Struct Eng 150(2):17.

Erikson RG, Gorman TM, Green DW, Graham D (2000) Mechanical grading of lumber sawn from small-diameter lodgepole pine, ponderosa pine, and grand fir trees from northern Idaho. Forest Prod J 50(7/8):59-65.

Graham RT, Harvey AE, Jain TB, Tonn JR (1999) The effects of thinning and similar stand treatments on fire behavior in western forests. General Technical Reports PNW-GTR-463. USDA Forest Service, Pacific Northwest Research Station, Portland, OR.

Hernandez R, Green DW, Kretschmann DE, Verrill SP (2005) Improved utilization of small-diameter ponderosa pine in glulam timber. Res. Pap. FPL-RP-625 US Department of Agriculture, Forest Service, Forest Products Laboratory. Madison, WI. 36 pp.

ICC (2018). International building code (IBC). Falls Church, Va. International Code Council.

Jahedi S, Muszynski L, Riggio M, Bhandari S (2020) Layup-App: A Python program developed to calculate CLT properties and to design custom layups. https://github.com/sina-jahedi/CLT_Design_Values_Calculator (15 February 2022).

Jahedi S, Muszynski L, Riggio M, Bhandari S (2022) MOE distribution in visually graded ponderosa pine lumber harvested from restoration programs in Southern Oregon and Northern California. Wood Fiber Sci 54(2): 75-80.

Jahedi S, Muszynski L, Riggio M, Bhandari S (2023) Integrity of melamine formaldehyde bonds in ponderosa pine cross-laminated timber. Isolating adhesive compatibility effect. For Prod J.

Khokhar A, Zhang H, Ridley-Ellis D, Moore J (2008) Determining the shear modulus of Sitka spruce from torsion tests. in Proceedings of the 10th World Conference on Timber Engineering, Miyazaki, Japan.

Kretschmann DE (2010) Mechanical properties of wood. In: Wood handbook: Wood as an engineering material. FPL-GTR-190; USDA Forest Service, Forest Products Laboratory, Madison, WI.

Kreuzinger H (1999) Platten, Scheiben und Schalen. Ein Berechnungsmodell fur. Bau mit Holz 1:34-39.

Larkin B (2017) Effective bonding parameters for hybrid cross-laminated timber (CLT). MS thesis, Oregon State University, Corvallis, OR. 184 pp.

Lawrence B (2017a) Utilization of low-value lumber from small-diameter logs harvested in Pacific Northwest Forest Restoration Programs in hybrid cross laminated timber (CLT) core layers: A market response. MS thesis, Oregon State University, Corvallis, OR. 114 pp.

Lawrence C (2017b) Utilization of low-value lumber from small-diameter timber harvested in Pacific Northwest Forest Restoration Programs in hybrid cross laminated timber (CLT) core layers: Technical feasibility. MS thesis, Oregon State University, Corvallis, OR. 166 pp.

Liao Y, Tu D, Zhou J, Zhou H, Yun H, Gu J, Hu C (2017) Feasibility of manufacturing cross-laminated timber using fast-grown small diameter eucalyptus lumbers. Constr Build Mater 132:508-515, doi: 10.1016/j.conbuildmat.2016.12.027.

Ma Y, Musah M, Si R, Dai Q, Xie X, Wang X, Ross RJ (2021) Integrated experimental and numerical study on flexural properties of cross laminated timber made of low-value sugar maple lumber. Constr Build Mater 280: 122508, doi: 10.1016/j.conbuildmat.2021.122508.

Mishra P, Pandey CM, Singh U, Gupta A, Sahu C, Keshri A (2019) Descriptive statistics and normality tests for statistical data. Ann Card Anaesth 22(1):67-72, doi: 10.4103/aca.ACA_157_18.

Mohamadzadeh M, Hindman D (2015) Mechanical performance of yellow-poplar cross laminated timber. Report No. CE/VPI-ST-15-13, Blacksburg, VA.

Rainville R, White R, Barbour J (2008) Assessment of timber availability from forest restoration within the Blue Mountains of Oregon. Gen Tec Rep PNW-GTR-752, US Department of Agriculture, Forest Service, Pacific Northwest Research Station, Portland, OR.

Samson M, Sotomayor-Castellanos J (1991) Constant bending method for determining modulus of elasticity of lumber in structural size. Wood Fiber Sci 23:520-532.

Schreier H, Orteu JJ, Sutton MA (2009) Image correlation for shape, motion and deformation measurements: Basic concepts, theory and applications. Springer Science & Business Media, Springer New York, NY.

Sigrist C, Lehmann M (2014) Potential of CLT produced from non-structural grade Australian *Pinus radiata*. *in* WCTE 2014 - World Conference on Timber Engineering, Proceedings. Quebec City, Canada.

Vaughan D, Auty D, Dahlen J, Meador AJS, Mackes KH (2021) Modelling variation in wood stiffness of *Pinus ponderosa* using static bending and acoustic measurements. Forestry 94(2):232-243, doi: 10.1093/forestry/cpaa030.